Preliminary Biological Evaluation of Powder-like Perovskite/Metal oxide Nanocomposite Developed by a Facile Wet-chemical Method

Sadia Gillani[1], Shan e Zahra[2], Mamoona Yasmeen[1], Azka Shahid Ejaz[1], Sajidullah Khan[1], Muhammad Abdul Basit [1,*],

[1]Department of Materials Science and Engineering, Institute of Space Technology, Islamabad, Pakistan
[2]Department of Physics, Institute of Space Technology, Islamabad, Pakistan
[*]Corresponding author: a.basit@ist.edu.pk

Abstract

In this study, $CsPbBr_3$ nano-powder was sonicated, and then an electrostatic self-assembly process was employed for coating them on TiO_2 to generate Perovskite/Metal Oxide as a nanocomposite (NC). Electron microscopy (SEM) was used to analyze perovskite nanoparticles' structural and morphological features. This investigation confirmed successful NC synthesis, since particle sizes and morphologies were properly determined. Along with various materials-based characterization, the biological effect of corresponding nano-powders (i.e., $CsPbBr_3$, TiO_2, and their NC) is determined and discussed to reveal the initial biotechnological features, including but not limited to cell viability. Moreover, the interaction between NC and Xanthomonas campestris-exposed tomato plants was analyzed, which reflected increased proline content, referring to the superior defense system of $TiO_2/CsPbBr_3$-treated plants against the aforementioned bacterium. $CsPbBr_3$ alone exhibited quite a lower proline level ($1.51mg/gFW$) of the corresponding plant as compared to TiO_2 ($2.23mg/gFW$), which fell in the range of effective values for$TiO_2/CsPbBr_3$ ($1.91mg/gFW$). Moreover, cell viability results also revealed the toxic nature of $CsPbBr_3$ from day 1 to day 3, cell viability percent reduced from 80% to 40% which can be reasonably reduced owing to its conjunction with TiO_2.

Keywords—Antibacterial activity, cesium lead bromide, proline, TiO_2

1 Introduction

Inorganic nanoparticles have gained a significance in modern material science, namely in biotechnology, due to their unique physical features. The two factors of inorganic nanoparticles lead to specific physical properties, which primarily encompass size-dependent optical, magnetic, electronic, and catalytic features [1]. Among these perovskite materials (PMs) with their distinctive ABX_3 crystal structure, there are notable properties, including nature, biocompatibility, anti-inflammatory and antibacterial activity, effective drug delivery, and bioactivity, which have contributed to an increase in biotechnological applications [2]. Nanoparticles have numerous applications across various sectors, including environmental science, agriculture, food technology, biotechnology, biomedicine, and pharmaceuticals, such as in the treatment of wastewater. Metal oxide nanoparticles, especially TiO_2, are extensively utilized be-cause of their remarkable thermal, optical, electrical, and magnetic properties. Titania is the most naturally occurring titanium oxide. TiO_2, which occurs colourless but highly reflective powder that typically exhibits hydrophobic properties under standard conditions [3]. To attain a higher level of stability in perovskite, multiple innovative strategies have been employed to tackle this significant challenge while preserving the remarkable luminescence properties. These strategies include surface capping and the incorporation of perovskite into organic or inorganic matrices [4]. Additionally, the combination of PMs and TiO_2 is unique for its diversity and technological uses in multiple applications, but not limited to photocatalysis [5] under real environmental conditions. Such NCs offer a wide range of sunlight absorbance, directly influencing the electron-hole (e-h) generation process, which further forms the basis for

ISSN: 2523-0379 (Online), ISSN: 1605-8607 (Print)
DOI: https://doi.org/10.52584/QRJ.2301.03

developing photocatalysts for solar cells or electrodes for fuel cells, etc. Various surface science methods have extensively investigated the photochemical mechanisms and basic principles of photocatalysis, especially in the last decade. Such e-h generation related to the formation of reactive oxygen species (ROS) serves as signaling molecules in plants and maintains physiological activities, as well as they also exhibit the tendency to harm living cells. [6] apart from their role to perform antibacterial activities in plants and animals. NPs like PMs may result in cytotoxicity, genotoxicity, and ecotoxicity due to ROS production as well. One of the main worldwide issues is antibiotic resistance, which makes conventional treatments and/or materials ineffective against many harmful bacteria. Affecting human and agricultural health, bacterial infections challenge food security and crop yield [7]. For instance, black rot of tomato plants brought on by the bacterial disease Xanthomonas Campestris makes farming challenging [8]. Environmental issues and bacterial resistance restrict the effectiveness of medicines and chemical insecticides. On the one hand, there is a need for new antibacterial methods and/or materials that are both sustainable and effective [9]. There is a need to investigate the harmful effects of the emerging NPs (used for photoactive applications such as TiO_2, perovskites, and their NCs). Recent studies show that PMs can produce ROS that inhibit bacterial biofilms and microbiological growth, making them promising antibacterial agents. Since perovskites and metal oxides have synergistic antibacterial effects, perovskite NCs can treat agricultural bacterial infections [8,9]; however, the presence of Pb, Cs, and Br, etc., is associated with carcinogenic effects too. Despite these advances, perovskite NCs are understudied biologically. In addition, there is an essential need to investigate more long-term and efficient alternatives to chemical treatments because of the serious risks they pose to human and environmental health. The development of antibacterial drugs based on nanomaterials (NMs) that target Xanthomonas Campestris in tomato plants is an area where a lot of knowledge remains required [10] [11] [12] [13] [14] [15].// Since we have recently reported the chemical and electrochemical performance of Perovskite/Metal oxide NCs [16] We importantly followed the biological influence of such materials where ROS generation is evident, and the biological entities, i.e., animals and/or plants, may be harmed/benefit from their exposure under light or in the dark. Definitely, the quantitative presence of such NPs plays a key role in such activities; nevertheless, our studies showed that the TiO_2, PMs, and the TiO_2/Perovskite NCs exhibit optimizable cell viability performance as well as antibacterial effect on diseased Tomato plants. In-depth materials-based analysis of all relevant NPs using imperative technical equipment such as FESEM, FTIR, EDS, etc., is reported in combination with preliminary biological testing.

2 Materials and Methods

All chemicals and salts required during the experimentation were used as received without any further processing. For this work, perovskite NCs were synthesized using the chemicals N-N Dimethylformamide (DMF) ($HCON(CH_3)_2$), Methanol (CH_3OH), Cesium Bromide ($CsBr$), Lead Nitrate ($Pb(NO_3)_2$), Acetic Acid (CH_3COOH), and 2-Propanol (C_3H_8O), and were purchased from Sigma Aldrich. Each of these chemicals was crucial to the experimental process, as it ensured proper dissolution, precursor supply, pH regulation, and purification.

2.0.1 Preparation of Solutions

Lead nitrate, $Pb(NO_3)_2$ salt is used as a cationic precursor for the adsorption of lead (Pb^{+2}) on TiO_2 (P-25) particles. To prepare 100 mL of 0.2 M $Pb(NO_3)_2$ solution, dissolve 6.62 g of $Pb(NO_3)_2$ in 100 mL of DMF. Stir thoroughly until all particles are dissolved in solvent, as illustrated in Fig. 1. Cesium bromide ($CsBr$) salt is used as an anionic precursor for the reaction of Cesium (Cs^{+1}) and anionic (Br^{-1}) on the surface of TiO_2 (P-25). To prepare 100 mL of 0.2 M $CsBr$ solution, dissolve 4.26 g of $CsBr$ in 100 mL of DMF. Place the solution on a hot plate and start magnetic stirring for 24 hours at $50°C$ [14,16].

2.0.2 Synthesis of $CsPbBr_3$ NPs

For the synthesis of $CsPbBr_3$, place the prepared $CsBr$ and $Pb(NO_3)_2$ solutions in a beaker with a 1:1 molar ratio. After a one to two-hour incubation period, stir the mixture. To ensure complete mixing without creating unwanted splashing or foaming, the pace of stirring should be moderate [11,16]. A yellow $CsPbBr_3$ precipitate should begin to develop as the mixture is being stirred. Until the precipitate production stops and the reaction is complete, keep stirring. Simply use the decantation method to filter the precipitate that results, then collect the particles in a petri dish and dry them in an oven at $60°C$ for several hours.

2.1 Synthesis of TiO_2/$CsPbBr_3$ NCs

For the deposition of TiO_2 NPs on $CsPbBr_3$ by adapting the method of M. Yasmeen et al. [14] we used methanol as a solvent for TiO_2 particle dissolution. First, 4g of TiO_2 particles were added to 140 mL of

methanol in a clean, dry beaker, and the mixture was stirred. In the next step, 0.4 g of $CsPbBr_3$, i.e, 1:10, was added to this solution. After that solution was placed on the magnetic stirrer for 40 min at $30°C$. In the following step, the solution is allowed to settle for 10 min and then centrifuged at 8000 rpm for 10 min. All the precipitates were settled down in centrifuge tubes, and decantation was done. In the last step, all the precipitates were collected in a petri dish, and they were allowed to air dry for 2 h. $TiO_2/CsPbBr_3$ perovskite NC has been effectively obtained.

3 Results and Discussion

3.1 Analysis of Nano Particles

The morphology, homogeneity, and size distribution of commercial TiO_2 (P25) particles were examined using Field Emission Scanning Electron Microscopy (FESEM) characterization techniques [11]. Li et al. showed different morphologies of $CsPbBr_3$ NPs [4]. In Fig. 2 (a), (b), and (d), the findings indicate that the particles exhibit a uniform size distribution. In FESEM images, small spherical particles are observed to be aggregated and separated. The results of the EDS study indicate that Ti and O elements are detected in all spectra [16]. Only the additional peak observed in the EDS full spectrum graph is attributed to platinum, employed in sputter coating. Apart from this, no impurities are detected as seen in Fig. 2(c). The size of the particles plays a crucial role in determining the characteristics and applications of nanoscale technology. ImageJ® and FESEM images serve as crucial tools for assessing size. In our study, we conducted an analysis of the particle size distribution presented in Figure 3.1(e) using ImageJ®. Our findings revealed variations reaching approximately 28 nm [17].

Wet-chemical synthesis typically produces spherical agglomerated $TiO_2/CsPbBr_3$ NC from solution-based synthesis. Fig. 3(a) and (b) show spherical particles with smooth surfaces at different magnifications, with a 500 nm scale bar [18]. The $TiO_2/CsPbBr_3$ NC was analysed using ImageJ®, depicting a particle size distribution graph. Fig. 3(c) shows that the resultant NC powder has particles sized between 42.73 to 60.89 nm. The ImageJ® graph confirms particle size changes, showing an average dimension of 47.98 nm. These powder particles are larger than pure TiO_2 (P-25) NPs indicating the presence/deposition $CsPbBr_3$ on TiO_2 particles [19]. FESEM analysis makes it impossible to detect cesium (Cs), lead (Pb), bromide (Br), titanium (Ti), and oxygen (O) atoms or their derivatives. FESEM-coupled EDS detects titanium, oxygen, cesium, lead, and bromine (Fig. 4). The 1 μm EDS spectrum of the $TiO_2/CsPbBr_3$ composite reveals its elemental composition, structural features, and potential contamination sources [20]. High oxygen levels indicate the existence of TiO_2, a key material component. The particles deposited are of a crystalline nature and have been reported elsewhere by our group previously [16].

After qualitative verification, FTIR characterization was done. The fingerprint groups from 400 to 1800 cm^{-1} and functional area from 1800 to 4000 cm^{-1} define the FTIR spectrum. Fig. 5(a) displays the $CsPbBr_3$ FTIR spectrum. The FTIR spectrum of $CsPbBr_3$ reveals peaks related to the perovskite's inorganic structure and possible manufacturing residue [21]. The presence of Cs-Br and Pb-Br stretching vibrations supports the $CsPbBr_3$ perovskite structure. C=0, N=0, and C-OH peaks suggest solvent or unreacted precursor organic pollutants. An oxidized sample has a Pb-O stretching peak at 420 cm^{-1}. $TiO_2/CsPbBr_3$ FTIR spectra are shown in Fig. 5(b). The spectrum peaks at 798 cm^{-1}, indicating the Ti-O-Ti bonds' vibrational absorption band [22]. In our situation, the peaks at 2853 and 2922 cm^{-1} indicate organic ligand signals on $CsPbBr_3$, caused by the solvent DMF [20]. Bare DMF has a C=0 bond strength of 1675 cm^{-1}. Compared to $CsPbBr_3$ and $CsPbBr_3/TiO_2$ NCs, the reduction in fundamental peaks at 2923 cm^{-1} suggests carbonaceous residue loss and dehydroxylation. The FTIR spectrum of the $TiO_2/CsPbBr_3$ composite indicates its chemical structure and composition. The peaks present throughout the manufacturing process are indicative of TiO_2, $CsPbBr_3$, and possible organic residues, i.e, DMF.

3.2 Cell Viability

Viability is the percentage of healthy, alive cells following chemical or environmental exposure. Cell viability evaluates NP effects on cell survival, proliferation, and function. Cytotoxicity, apoptosis, and biocompatibility are tested on NPs. Due to their tiny size and high surface area, NPs interact with biological structures differently than larger particles. This combination may be physiologically advantageous or toxic. NPs-based imaging and medicine delivery can be developed using cell viability tests measured by MTT assay [23]. Summarizing it, Fig. 6 shows cell viability of all samples on days 1 and 3. The harmful effects of $TiO_2/CsPbBr_3$ and $CsPbBr_3$ NPs as evidenced by a significant decrease in cell viability from day 1 to day 3 in Fig. 6 (a, b) [24]. It is evident that there was a significant decrease in the cell viability level of osteoblasts whose

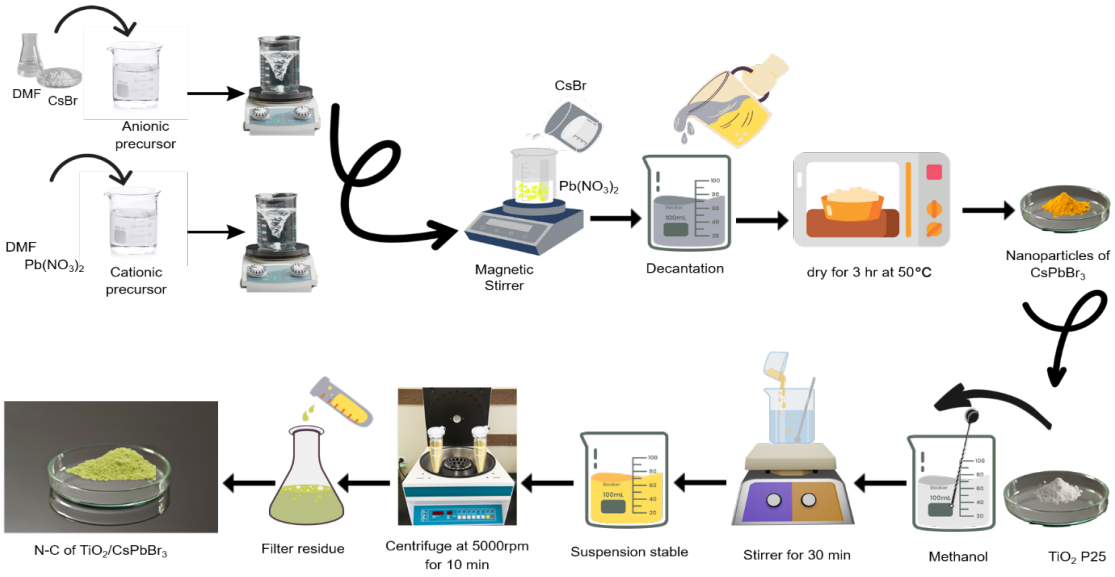

Fig. 1: Development of $TiO_2/CsPbBr3nanocomposite$

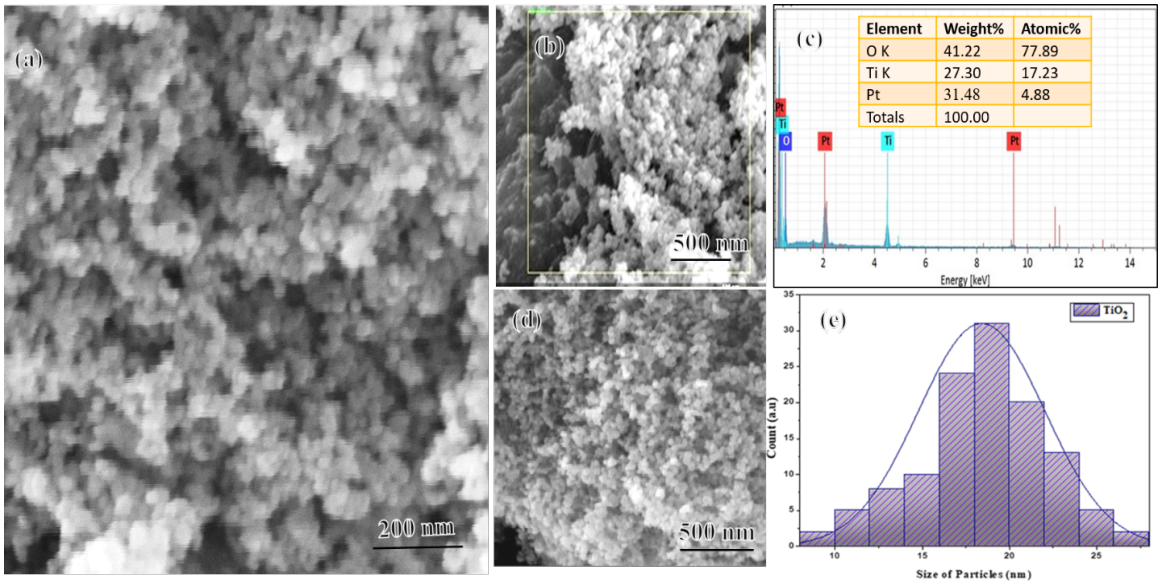

Fig. 2: FESEM images and EDS images of TiO_2 (P-25) nanoparticles, (a) at 200 nm, (b) at 500 nm full spectrum, (c) full area EDS, (d) at 500nm, (e) particle size analysis of $_{T}iO2$

initial density was 20 x 105 (normalized as 100%) and compared with the various samples treated by corresponding NPs. Having determined the cell density of various suspensions taken from respectively treated cell (50 micro liter) suspensions after day 1 and day 3 (the samples were meanwhile incubated at about 35-37 degrees Celsius), it was seen that the TiO_2 and PMs ($CsPbBr_3$) had less effect on the cell than the NC. This influence became severe on day 3, where the cell viability decreased to a significant level of ¡50%, indicating the harmfulness of overexposure to such nanoscale $TiO_2/CsPbBr_3$ powder. It is evident that this multiplied response of corresponding NP is mainly induced from the PMs, i.e., $CsPbBr_3$, which is capable of producing e-h and thus ROS for any such activity. The e-h generation that was previously affirmed by Mamoona et al. [14] in such a case may produce harmful biological effects if not optimized in terms of exposure (i.e., number of days) and/or quantity. It is to reiterate that stable cells have NP resistance or cytotoxic saturation [25] as well, and cells can adapt by increasing antioxidant enzymes, efflux pump activity, autophagy, or DNA repair. Bioavailability, cytotoxicity, and cell death can be reduced by NPs agglom-

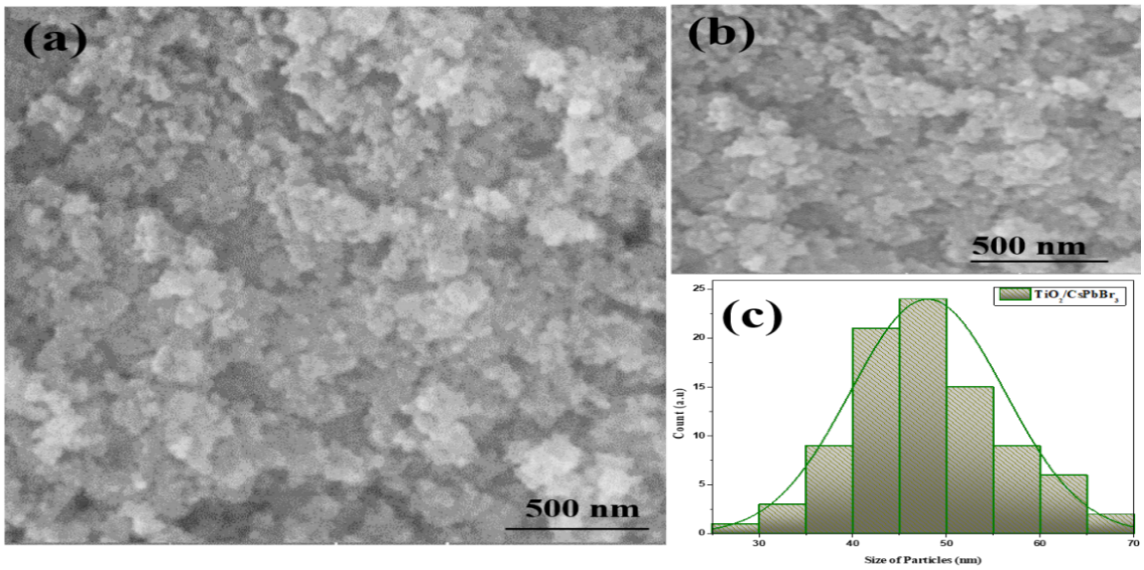

Fig. 3: FESEM images of $TiO_2/CsPbBr_3$ at (a) 50kx, (b) 100kx (c) particle size analysis

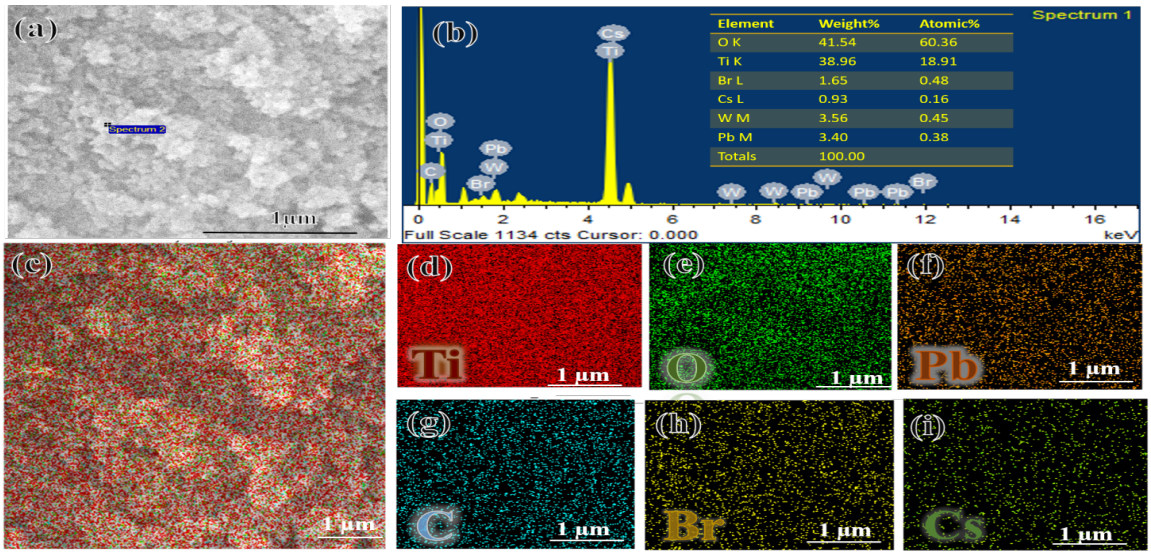

Fig. 4: EDS Elemental Area Mapping of $TiO_2/CsPbBr_3$ N-C showing (a) electron image (b) percentage composition, (c) overall distribution, distribution of (d) Ti, (e) O, (f) Pb, (g) C, (h) Br and (i) Cs

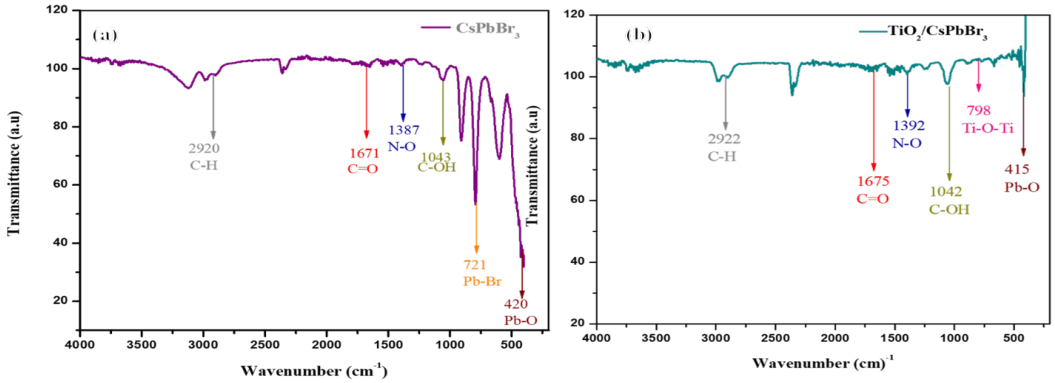

Fig. 5: FTIR spectrum of. i.e., (a)$CsPbBr_3$ (b) $TiO_2/CsPbBr_3$

eration or disintegration. Our results show that most of the sensitive cells have died, and the remaining cells are more resistant to NPs in the mentioned order TiO_2 ¿ $CsPbBr_3$ ¿ $TiO_2/CsPbBr_3$, indicating cytotoxic activity [26]. Based on these findings, it is inferred that initially (after day 1), the $TiO_2/CsPbBr_3$ powder was active alone owing to the synergetic effect of oxide/bromide materials in it, which further became more active (after day 3) due to the slower activation (and/or ROS generation tendency) of TiO_2 and $CsPbBr_3$ alone, as depicted in Fig. 6(b).

4 Plant-based Antibacterial Activity

4.0.1 Determination of Proline

To calculate the proline content in diseased plants firstly, Dissolve 3g suphosalicylic acid in 50mM phosphate buffered saline (PBS) having pH 7.8 to make final volume 100ml then take 40.933 ml 85% H3PO4 and make the final volume 100ml in last step, take 60ml pure acetic acid mix with 40ml (6M H3PO4), then add 2.5g Ninhydrin and give water bath at $7°C$ avoid the solution from light, store at $4°C$. Repeated this method three times to avoid any error.

4.0.2 Reaction Methodology

Take a dry sample, cut it into small pieces, approximately 0.1gm in tubes with a stopper, then add 5ml of 3% sulpho-salicylic acid solution and incubate in boiling water at $100°C$ for 10 minutes. Cool down the samples in tap water and then take 1ml supernatant in clean tubes with a stopper, add 1ml pure acetic acid, also add 1.5ml Ninhydrin solution, shake the samples, and again give a boiling water bath at $100°C$ for 40 minutes. Cool down the samples in tap water, add 2.5ml pure toluene and shake intensively, allow the samples to settle down for a few minutes, finally read the supernatant spectrophotometrically at OD520. Set zero with pure toluene. Proline content is determined by using the formula $(\mu g/gFW) = \frac{C.V}{\frac{A}{W}}$

Here,

C: proline content calculated from the standard curve

V: volume of supernatant used to extract proline i.e., 5ml

A: volume of supernatant used, i.e. 1ml

W: sample wt.

4.0.3 Treatment with NPs

In contrast to the previously reported antibacterial performance [14],We opted for a new route to expose the effect of $TiO_2/CsPbBr_3$ NC or its constituent particles against a bacterium. We involved a foliar approach, which associated the direct application of an NPs solution onto the leaves of tomato plants having any bacterial disease (i.e., Black rot) [4,5]. The NPs are applied onto the leaves in a suspension form and sprayed in a standard way, allowing them to come into contact with the plant surface and perhaps impede the proliferation of bacterial diseases [27]. Fine mist sprayers are used to cover the leaf surface uniformly. NPs in nanofluids enter plant tissues and adhere to leaf surfaces, where they kill bacteria by creating ROS or directly interacting with the bacterial membrane, as illustrated in Fig. 7(a). To evaluate antibacterial performance, the stress is measured by plant tissue proline levels using the calorimetry method [28], [29], [30]. Stress-induced proline accumulation in plants. Specifically, bacterial infections cause biotic stress. After spraying NPs, leaf samples are chemically treated to extract proline. This procedure continues until the desired material is obtained. A colorful complex is formed by the proline and ninhydrin reaction. This happens in acid. Proline content impacts spectrophotometer color intensity at 520 nm, and plant stress is measured accordingly, which is depicted in Fig. 7(b). It was observed that stress-induced proline accumulated in tomato plants infected with Xanthomonas campestris. Healthy plants have low proline levels of 1.83 mg/g (FW), suggesting little stress. Proline levels rose to 2.53 mg/g (FW) in diseased plants, indicating stress from the bacterial infection. TiO_2 NP treatment re-duced proline accumulation to 2.23 mg/g (FW) despite greater stress than in healthy plants [29]. This suggests that NPs relieve stress by partially preventing/harming bacteria. When $TiO_2/CsPbBr_3$ NC is employed, proline dropped to 1.91 mg/g (FW), which implied effective control/harm by the corresponding powder. This combined therapy approach increases healthy plant proline levels, suggesting better bacterial control and stress reduction. $CsPbBr_3$ NPs reduce proline to 1.51 mg/g (FW), below the level for a healthy plant, emphasizing that the combination of TiO_2 and $CsPbBr_3$ may play a more advantageous role in controlling any such disease. It also suggests that $CsPbBr_3$ NPs decrease stress more than the combination treatment, which may not be beneficial to healthy plants [30]. Stress helps plants activate their natural defenses, stay resilient, and operate properly. While mild stress can activate defense mechanisms, excessive stress impairs function; thus, reducing it is beneficial.

5 Conclusion

This study reports the effective synthesis of TiO_2, $CsPbBr_3$, and $TiO_2/CsPbBr_3$ NPs by the use of an

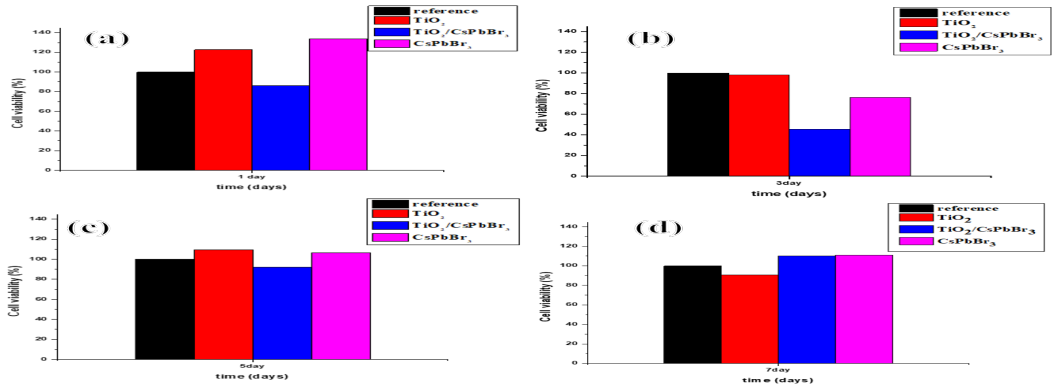

Fig. 6: Cell viability of all samples on (a) day 1 and (b) day 3

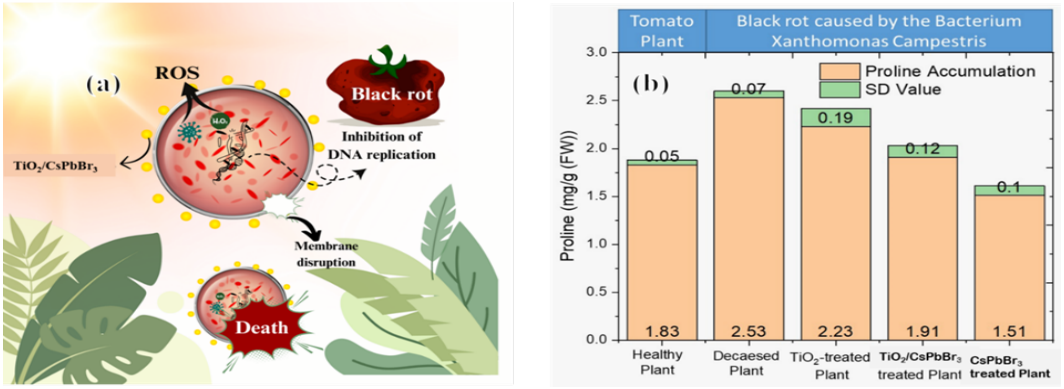

Fig. 7: (a) Antibacterial mechanism of black rot in tomato plants, (b) Antibacterial evaluation of NCs on tomato plants using proline assessment

electrostatic self-assembly approach. Evaluation shows that having such PMs in NCs is capable of controlling bacterial growth in plants; however, a precise optimization of their quantity and exposure is suggested owing to the detrimental cell viability results corresponding to 3 days' exposure of $TiO_2/CsPbBr_3$ and its constituents to osteoblasts. Corresponding morphology is shown by FESEM, whereas EDS peaks only show Cs, Pb, and Br. FTIR spectra show organic residues such as DMF. Peaks at 2923 cm^{-1} suggested organic ligands, whereas Ti-O-Ti bonds appeared at 798 cm^{-1}. NPs as well as NC tested for antibacterial action on Xanthomonas Compestris (that causes black rot in tomato plants) suggest the optimizable proline accumulation in leaves, referring to the potential of its use for agricultural sprays. Nevertheless, it must be taken into account of the presence of Pb.

References

[1] P. Thakur and A. Thakur, "Introduction to Nanotechnology," in *Synthesis and Applications of Nanoparticles*, Singapore: Springer Nature Singapore, 2022, pp. 1–17.

[2] K. A. Altammar, "A review on nanoparticles: characteristics, synthesis, applications, and challenges," *Frontiers in Microbiology*, vol. 14, p. 1155622, Apr. 2023.

[3] V. Verma, M. Al-Dossari, J. Singh, M. Rawat, M. G. M. Kordy, and M. Shaban, "A review on green synthesis of TiO_2 NPs: photocatalysis and antimicrobial applications," *Polymers*, vol. 14, no. 7, p. 1444, Apr. 2022.

[4] W. Li *et al.*, "Ethanol–water-assisted room-temperature synthesis of $CsPbBr_3/SiO_2$ nanocomposites with high stability in ethanol," *Journal of Materials Science*, vol. 54, no. 5, pp. 3786–3794, Mar. 2019.

[5] P. Thakur and A. Thakur, "Nanomaterials, their types and properties," in *Synthesis and Applications of Nanoparticles*, Singapore: Springer Nature Singapore, 2022, pp. 19–44.

[6] V. Takhar and S. Singh, "Nanomaterials ROS: A comprehensive review for environmental applications," *Environmental Science: Nano*, vol. 12, no. 5, pp. 2516–2550, 2025.

[7] A. Kaphle, P. N. Navya, A. Umapathi, and H. K. Daima, "Nanomaterials for agriculture, food and environment: applications, toxicity and regulation," *Environmental Chemistry Letters*, vol. 16, no. 1, pp. 43–58, Mar. 2018.

[8] A. Varympopi *et al.*, "Antibacterial activity of copper nanoparticles against *Xanthomonas campestris* pv. *vesicatoria* in tomato plants," *International Journal of Molecular Sciences*, vol. 23, no. 8, p. 4080, Apr. 2022.

[9] M. Ahmad *et al.*, "Optimization of SiO_2–TiO_2 nanocomposite in hole transporting layer (PEDOT:PSS) for enhanced performance of planar Si-based hybrid solar cells,"

International Journal of Energy Research, vol. 46, no. 7, pp. 9863–9874, Jun. 2022.

[10] M. Karami, M. Ghanbari, O. Amiri, and M. Salavati-Niasari, "Enhanced antibacterial activity and photocatalytic degradation of organic dyes under visible light using cesium lead iodide perovskite nanostructures prepared by hydrothermal method," *Separation and Purification Technology*, vol. 253, p. 117526, Dec. 2020.

[11] M. A. Abbas, M. A. Basit, M. Ali, M. Lee, T. J. Park, and J. H. Bang, "Atomic layer deposition of sulfur-defective ZnS on TiO_2: tailoring optical and electronic properties for visible-light-driven water splitting," *Applied Surface Science*, vol. 687, p. 162314, Apr. 2025.

[12] J. R. Gonzalez-Moya, C.-Y. Chang, D. Radu, and C.-Y. Lai, "Photocatalytic deposition of nanostructured $CsPbBr_3$ perovskite quantum dot films on mesoporous TiO_2 and their enhanced visible-light photodegradation properties," *ACS Omega*, vol. 7, no. 30, pp. 26738–26748, Aug. 2022.

[13] E. Afanaseva, V. Klinkov, E. Vaishlia, V. Andreeva, Z. Patrakov, and M. Gushina, "The synthesis of $CsPbBr_3$ and $CsPbBr_3/Cs_4PbBr_6$ nanoparticles," in *Proc. 2022 Int. Conf. on Electrical Engineering and Photonics (EExPolytech)*, St. Petersburg, Russia: IEEE, Oct. 2022, pp. 207–209.

[14] M. Yasmeen *et al.*, "Effective development and utilization of SILAR-assisted TiO_2 and $CsPb_2Br_5$ nanocomposites for photochemical and biological cleaning of environment," *Ceramics International*, vol. 50, no. 12, pp. 21253–21264, Jun. 2024.

[15] A. Pravin, K. Ramesh, R. Kaushik, and S. Srivignesh, "Nanotechnological applications in horticultural plant disease management," in *Futuristic Trends in Chemical Material Sciences & Nanotechnology, Vol. 3, Book 4*, M. Sudhanan *et al.*, Eds., Iterative International Publishers, 2024, pp. 80–102.

[16] T. Ohno, K. Sarukawa, K. Tokieda, and M. Matsumura, "Morphology of a TiO_2 photocatalyst (Degussa P-25) consisting of anatase and rutile crystalline phases," *Journal of Catalysis*, vol. 203, no. 1, pp. 82–86, Oct. 2001.

[17] R. Theissmann, C. Drury, M. Rohe, T. Koch, J. Winkler, and P. Pikal, "Comparative electron microscopy particle sizing of TiO_2 pigments: sample preparation and measurement," *Beilstein Journal of Nanotechnology*, vol. 15, pp. 317–332, Mar. 2024.

[18] Y. Liu *et al.*, "Nano ball milling using titania nanoparticles to anchor cesium lead bromine nanocrystals and energy transfer characteristics in TiO_2@$CsPbBr_3$ architecture," *Small*, vol. 16, no. 40, p. 2004126, Oct. 2020.

[19] P. Nuket, "Stability enhancement of $CsPbBr_3$ quantum dots by coating TiO_2 as a surface encapsulation," M.Eng. thesis, Chulalongkorn University, Bangkok, Thailand, 2020.

[20] Y.-K. Ren *et al.*, "Controllable intermediates by molecular self-assembly for optimizing the fabrication of large-grain perovskite films via one-step spin-coating," *Journal of Alloys and Compounds*, vol. 705, pp. 205–210, May 2017.

[21] J. Mei, F. Wang, Y. Wang, C. Tian, H. Liu, and D. Zhao, "Energy transfer assisted solvent effects on $CsPbBr_3$ quantum dots," *Journal of Materials Chemistry C*, vol. 5, no. 42, pp. 11076–11082, 2017.

[22] Z. Ge, A. Yin, M. Fang, W. Zhu, and C. Li, "SiO_2@TiO_2–$CsPbBr_3$ hierarchical microspheres for dye-sensitized solar cells to enhance photovoltaic conversion efficiency," *Journal of Materials Science: Materials in Electronics*, vol. 35, no. 17, p. 1183, Jun. 2024.

[23] M. H. Nawaz *et al.*, "Rosemary-loaded xanthan coatings on surgical-grade stainless steel for potential orthopedic applications," *Progress in Organic Coatings*, vol. 186, p. 107987, Jan. 2024.

[24] S. M. Mousavi *et al.*, "Data on cytotoxic and antibacterial activity of synthesized Fe_3O_4 nanoparticles using *Malva sylvestris*," *Data in Brief*, vol. 28, p. 104929, Feb. 2020.

[25] C. Liao, Y. Li, and S. C. Tjong, "Bactericidal and cytotoxic properties of silver nanoparticles," *International Journal of Molecular Sciences*, vol. 20, no. 2, p. 449, Jan. 2019.

[26] I.-S. Kim, M. Baek, and S.-J. Choi, "Comparative cytotoxicity of Al_2O_3, CeO_2, TiO_2 and ZnO nanoparticles to human lung cells," *Journal of Nanoscience and Nanotechnology*, vol. 10, no. 5, pp. 3453–3458, May 2010.

[27] J. Narware *et al.*, "Enhancing tomato growth and early blight disease resistance through green-synthesized silver nanoparticles: insights into plant physiology," *South African Journal of Botany*, vol. 166, pp. 676–689, Mar. 2024.

[28] M. F. El-Banna and A. Mosa, "Exogenous application of proline mitigates deteriorative effects of salinity stress in NFT closed-loop system: an ultrastructural and physio-biochemical investigation on hydroponically grown tomato (*Solanum lycopersicon* L.)," *Scientia Horticulturae*, vol. 330, p. 113061, Apr. 2024.

[29] A. S., R. M., and J. J. M., "*Piriformospora indica*-colonization in tomato seedlings enhances water stress tolerance by inducing antioxidant enzyme activities and proline accumulation," *Environment and Ecology*, vol. 41, no. 4C, pp. 2805–2813, Dec. 2023.

[30] B. Parra-Torrejón *et al.*, "Multifunctional nanomaterials for biofortification and protection of tomato plants," *Environmental Science & Technology*, vol. 57, no. 40, pp. 14950–14960, Oct. 2023.